










Carbon Chain Depletion of 2I/Borisov

Theodore Kareta¹ , Jennifer Andrews² , John W. Noonan¹ , Walter M. Harris¹ , Nathan Smith², Patrick O'Brien¹, Benjamin N. L. Sharkey¹, Vishnu Reddy¹ , Alessondra Springmann¹, Cassandra Lejoly¹, Kathryn Volk¹ , Albert Conrad³ , and Christian Veillet³

¹Lunar and Planetary Laboratory, Tucson, AZ, USA

²Steward Observatory, Tucson, AZ, USA

³Large Binocular Telescope Observatory, Tucson, AZ, USA

Received 2019 October 8; revised 2019 December 13; accepted 2019 December 17; published 2020 February 3

Abstract

The composition of comets in the solar system comes in multiple groups thought to encode information about their formation in different regions of the outer protosolar disk. The recent discovery of the second interstellar object, 2I/Borisov, allows for spectroscopic investigations into its gas content and a preliminary classification of it within the solar system comet taxonomies to test the applicability of planetesimal formation models to other stellar systems. We present spectroscopic and imaging observations from 2019 September 20 through October 26 from the Bok, MMT telescope (formerly the Multiple Mirror Telescope, Mount Hopkins, Arizona), and Large Binocular Telescopes. We identify CN in the comet's spectrum and set precise upper limits on the abundance of C₂ on all dates in October. We use a Haser model to convert our integrated fluxes to production rates and find $Q(\text{CN}) = (1.1\text{--}1.9) \times 10^{24}$ mols s⁻¹ increasing over 2019 October 1 to 26, consistent with contemporaneous observations. We set our lowest upper limit on a C₂ production rate, $Q(\text{C}_2) < 1.6 \times 10^{23}$ mols s⁻¹ on 2019 October 10. The measured upper limit ratio for that date $Q(\text{C}_2)/Q(\text{CN}) < 0.1$ indicates that 2I/Borisov is strongly in the (carbon-chain) “depleted” taxonomic group if there is any C₂ production at all. Most “depleted” comets are Jupiter-family comets (JFCs), perhaps indicating a similarity in formation conditions between the most depleted of the JFCs and 2I/Borisov. More work is needed to understand the applicability of our knowledge of solar system comet taxonomies onto interstellar objects and we discuss future work that could help to clarify the usefulness of the approach.

Unified Astronomy Thesaurus concepts: Spectroscopy (1558); Comets (280); Molecular gas (1073); Abundance ratios (11)

Supporting material: data behind figure

1. Introduction

The modern composition and structure of solar system comets retain information about conditions of the early protosolar disk from which they formed (Duncan et al. 1987; Bar-Nun & Kleinfeld 1989; Mumma et al. 1993; A'Hearn et al. 2012). Telescopic surveys of comet molecular abundances (A'Hearn et al. 1995; Fink 2009; Cochran et al. 2012) have revealed there to be multiple taxonomic classes of solar system comets whose differences are likely tied to differences in disk chemistry. Dynamical work also suggests multiple formation regions inside the disk (Biver & Bockelée-Morvan 2015; Dones et al. 2015; Bockelée-Morvan & Biver 2017; Meech et al. 2017) related to the modern dynamical classes of comets (Jupiter-family, Halley-type, long-period, etc.). Connections between dynamical class and composition (“normal,” carbon-chain depleted, carbon-chain and NH₂ depleted, etc.) have also been identified (A'Hearn et al. 1995; Fink 2009; Cochran et al. 2012) using spectroscopy of cometary comae. Spectroscopic observations of an active cometary coma, whether the object is from our solar system or interstellar, thus investigates the link between disk properties and produced planetesimals, and provides constraints on models of planetesimal and planet formation.

The discovery of the second-ever interstellar object comet 2I/Borisov on 2019 August 30 (MPEC 2019-R106)⁴ presents a

unique opportunity to contrast planetesimal formation in our solar system with formation processes in other stellar systems—in a way not possible with the first interstellar object found, 1I/'Oumuamua. 'Oumuamua is red with a pronounced elongation (Knight et al. 2017; Meech et al. 2017; Fitzsimmons et al. 2018; Trilling et al. 2018; Ye et al. 2018) with an assumed low, but undetermined, visible (<0.15) and infrared (<0.2) albedo (Fitzsimmons et al. 2018; Trilling et al. 2018) in a non-principal axis (“tumbling”) rotational state (Belton et al. 2018; Drahus et al. 2018; Fraser et al. 2018). There is strong evidence for nongravitational acceleration (Micheli et al. 2018). No gas emissions were detected from 'Oumuamua: chemical analyses were limited to observing its surface reflectivity (Fitzsimmons et al. 2018) and are consistent with an outer solar system body with appreciable organic content. All of these properties contrast with 2I/Borisov; the object's substantial outgassing provides more data about its formation, thermal history, and chemistry.

We summarize the currently known properties of 2I/Borisov. Its eccentricity and inclination are 3°31' and 44°1', respectively (JPL Orbit Solution #11, queried for 2019 October 1.0). Due to its low solar elongation angle it is visible only in the early morning, presenting a brief observing window. Guzik et al. (2019) obtained *g'*- and *r'*-band images with Gemini North, finding 2I/Borisov's color to be indistinguishable from solar system comets. de León et al. (2019) reported a red slope between 0.55 and 0.90 μm similar to D-type asteroids and cometary nuclei. Fitzsimmons et al.

⁴ <https://www.minorplanetcenter.net/mpec/K19/K19RA6.html>

Table 1
Observing Circumstances for 2I/Borisov

Telescope	Date	R_H (au)	Δ (au)	Time (UTC)	Airmass	T_{Exp} (s)	R (or filter)	Conds.
Bok (2.3 m)	Sep 20	2.67	3.25	12:07–12:17	1.89	600	1045	Photometric
MMT (6.5 m)	Oct 1	2.50	3.00	11:47–11:53	1.87–1.93	2×300	740	Cirrus?
...	Oct 9	2.41	2.84	11:46–12:06	1.75–1.82	4×300	740	Cirrus?
LBT ($2 \times 8.4\text{m}$)	Oct 10	2.39	2.82	12:00–12:16	1.57–1.64	2×500	2000	Photometric
Bok (2.3 m)	Oct 26	2.23	2.52	12:19–12:29	1.46	1200	HB CN Filter	Photometric

Note. Airmasses listed are for the start of each exposure.

(2019) detected CN emission from 2I/Borisov ($Q \sim 4 \times 10^{24}$ molecules s^{-1}) at a level appearing typical for comets at similar heliocentric distances. Fitzsimmons et al. (2019) also constrained the C_2 production ($Q < 4 \times 10^{24}$ molecules s^{-1}) and estimated water production by proxy ($Q \sim 1.7 \times 10^{27}$ molecules s^{-1}). McKay et al. (2019) derived from the 6300 Å [OI] line a water production rate of $\sim 6.3 \times 10^{26}$ mols s^{-1} , which could be high or typical compared to solar system comets depending on size estimated (Jewitt & Luu 2019).

Carbon “typical” comets have production rate ratios of C_2/CN of 0.66–3.0 (A’Hearn et al. 1995; Cochran et al. 2012), while comets with less C_2 are called “depleted.” Fitzsimmons et al. (2019) cannot discriminate 2I/Borisov between “typical” and “depleted” for 2I/Borisov, though the detection of CN does effectively rule out an uncommon composition like that of Comet Yanaka (1988r; Fink 1992) or 96P/Machholz (Schleicher 2008). Opatom et al. (2019) found no evidence of C_2 in their spectroscopic observations, suggesting moderate-to-strong ($\text{C}_2/\text{CN} < 0.3$) carbon-chain depletion. Spectroscopic observations can place chemical constraints on 2I/Borisov, allowing insight into another solar system’s disk chemistry and formation history by examination of the interstellar comet’s C_2 and CN abundance in ways that 1I/’Oumuamua could not.

2. Observations and Data Reduction

We observed interstellar comet 2I/Borisov on 2019 September 20 with the Boller & Chivens spectrograph at the 2.3 m Bok telescope (Kitt Peak National Observatory, Arizona), on 2019 October 1 and 9 with the Blue Channel spectrograph at the 6.5 m MMT telescope (Mount Hopkins, Arizona; Hastie & Williams 2010), and on 2019 October 10 with MODS on the Large Binocular Telescope (LBT; Pogge et al. 2006) to search for and measure the abundance of molecular species as well as to measure the reflective properties of dust in the object’s coma. We also imaged Borisov in the Hale–Bopp CN (Farnham et al. 2000) and Sloan r' filters on 2019 October 26 with the 90 Prime imager (Williams et al. 2004) on the Bok telescope. Observational details, including heliocentric and geocentric distances, spectral resolution, and exposure times among other information, are listed in Table 1. For context, our Bok observations took place approximately 7 hr after Fitzsimmons et al. (2019).

These spectra and images were reduced using standard techniques, including bias subtraction, flat-fielding, cosmic-ray rejection, local sky subtraction, and extraction of one-dimensional spectra. The spectra had wavelength solutions derived using comparison with helium–neon–argon lamps, had a standard extinction correction applied, and were flux-calibrated by comparison with nearby flux standard stars observed just beforehand. For the spectroscopic observations extracted apertures were chosen to maximize the comet signal

for each instrument and slit. For the data from 2019 September 20, this was an $18''.33$ (spatial) by $1''.5$ (slit width) box, 2019 October 1 had $15''.575$ by $1''.0$, 2019 October 9 had $26''.0$ by $1''.5$, and 2019 October 10 had $18''$ by $2''.4$. The imaging data were extracted using circular aperture photometry with a radius of $25''.0$ and largely followed the reduction procedure outlined in Farnham et al. (2000) using the dust reflectance slope measured from our 2019 October 10 spectrum. The standard star used (HD 81809) is noted in that work to be less than ideal for blue/UV observations, so we have overestimated errors when possible. We note that for the 2019 September 20 and October 1 data sets, insufficient data were collected to allow a median combination of spectra, making the two data sets “look” even noisier than their later counterparts even though cosmic rays were cleaned from them.

3. Analysis, Modeling, and Results

In order to search for molecular emission features, it is necessary to produce a flux-calibrated solar spectrum fit to subtract from the flux-calibrated data. This process creates a dust reflectance spectrum for the comet, which can be used to look for a spectral slope. The solar spectrum was taken from Chance & Kurucz (2010) and binned to the resolution of each data set. The original flux-calibrated spectra, best-fit reflectance, and dust-subtracted comet spectra are shown in Figure 1. The noisiness of the Bok data prevents a high-quality solar reflectance subtraction, while the later data become very linear after subtraction indicating a relatively good fit of the solar spectrum to the continuum points.

We consider the spectral slope between the blue, green, and red continuum regions defined for the Hale–Bopp filter set (Farnham et al. 2000) to compare reflectance slopes with other workers. These filters are centered at 4450, 5260, and 7128 Å, respectively. If we normalize our highest-quality data from 2019 October 10 at the green continuum point, then we find the blue-to-green slope to be $S' = 22 \pm 4\%$ /micron, and the green-to-red slope to be $S' = 11 \pm 3\%$ /micron. Fitzsimmons et al. (2019) suggested that the dust might be “redder” at shorter wavelengths, and our best data support that conclusion.

After the reflected sunlight from dust was subtracted, we searched for emission from molecules in the coma of 2I/Borisov (Table 2). For each possible feature we subtracted a linear estimate of the background as determined by a fit to data on either side of the feature and then integrated using a trapezoidal method all flux above it. That retrieved flux is compared against an upper limit found through the method described in Cochran et al. (2012), whereby a fraction of the local spectral noise is multiplied over the width of the bandpass that the feature was integrated over to determine blindly if the feature is “real.” All retrieved fluxes and upper limits are in Table 2.

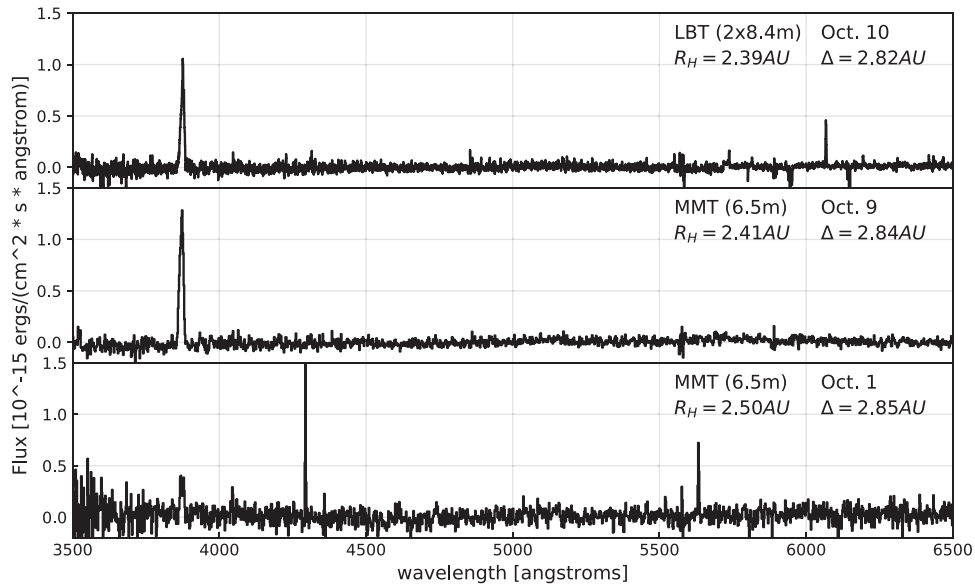


Figure 1. Spectral observations of 2I/Borisov. The flux-calibrated and dust-subtracted spectra of all three nights of spectroscopy from 2019 October. The heliocentric and geocentric distances are listed underneath the telescope names and dates on the figure. The same background and background-subtraction process was applied to all data sets. The CN B–X (0–0) band centered at 388.3 nm can be seen clearly in the MMT and LBT data.

(The data used to create this figure are available.)

Table 2
Fluxes and Production Rates of Cometary Molecules

Telescope	Flux (CN; erg/s*cm ²)	Flux (C ₂ ; erg/s*cm ²)	Q(CN; mol/s)	Q(C ₂ ; mol/s)	Q(C ₂)/Q(CN)
Bok (Sep 20)	<1.6 * 10 ⁻¹⁴	<1.8 * 10 ⁻¹⁴	<5.0 * 10 ²⁴	<8.0 * 10 ²⁴	...
MMT (Oct 1)	(2.9 +/- 0.4) * 10 ⁻¹⁵	<4.4 * 10 ⁻¹⁵	(1.1 +/- 0.2) * 10 ²⁴	<2.5 * 10 ²⁴	<2.3
MMT (Oct 9)	(9.9 +/- 0.5) * 10 ⁻¹⁵	<1.8 * 10 ⁻¹⁵	(1.74 +/- 0.09) * 10 ²⁴	<4.4 * 10 ²³	<0.3
LBT (Oct 10)	(1.22 +/- 0.03) * 10 ⁻¹⁴	<8.0 * 10 ⁻¹⁶	(1.73 +/- 0.04) * 10 ²⁴	<1.6 * 10 ²³	<0.1
Bok (Oct 26)	(3.8 +/- 0.7) * 10 ⁻¹³		(1.9 +/- 0.3) * 10 ²⁴

The CN B–X (0–0) band near 3883 Å is a relatively narrow two-peaked feature that we integrated from 3861 to 3884 Å based on the extent of the feature as calculated in Schleicher (2010). We detect CN strongly on 2019 October 1, 9, and 10, but the detection on 2019 September 20 is marginal, as background subtraction was challenging so close to the edge of the detector. We thus list it in Table 2 as an upper limit, but if it were a detection, the value should be similar to the value listed.

The C₂ Swan band ($\Delta\nu = 0$), with a bandhead at 5167.0 Å, is a much broader feature stretching over 200 Å in wavelength. The overall shape of the band has a sharp peak near the primary 0–0 bandhead and a secondary peak near 5129 Å at the 1–1 bandhead. We integrate from 5067 Å to the 0–0 bandhead at 5167 Å and to match the procedures of Fitzsimmons et al. (2019) and Opitom et al. (2019). There is no C₂ seen above the noise in any of the data. Detailed sections of the 2019 October 1, 9, and 10 spectra of 2I/Borisov show the CN detections and C₂ nondetections on those dates (Figure 2). For the 2019 October 10 data, we also measured upper limits over other ranges. If we integrate from the 0–0 bandhead to the 1–1 bandhead (5129–5167 Å), we get 39% of the 100 Å upper limit, and if we integrate over the full 200 Å, then we get 218% of the 100 Å upper limit. This is consistent with there being no variation in spectral properties or noise throughout the bandpass.

To convert the integrated fluxes to production rates, we used a standard Haser model (Haser 1957) with scale lengths and lifetimes from A’Hearn et al. (1995) and outflow velocity from Cochran & Schleicher (1993). We note that the A’Hearn et al. scale lengths and lifetimes assume a different outflow velocity, though this does not change inferred production rate ratios. The g -factor (formally the fluorescence efficiency) for C₂ was taken from A’Hearn et al. (1995) and the g -factor for CN was taken from Schleicher (2010) for the appropriate heliocentric distance and velocity on each date. The lifetimes increased proportional to heliocentric distance squared and the g -factors were scaled down by the same factor. We have verified the output of our Haser model implementation by comparison of its output with a recent paper on the topic, Hyland et al. (2019). The input fluxes and output production rates for all nights are presented in Table 2. The production rate ratio upper limit, $Q(C_2)/Q(CN)$, is measured as <0.1, which indicates that 2I/Borisov is clearly in the “depleted” group of the A’Hearn et al. (1995) taxonomy if there is any C₂ at all. A comparison of our inferred $Q(C_2)/Q(CN)$ ratio with those of the A’Hearn et al. (1995) sample as submitted to the Planetary Data System in 2003 (Osip et al. 2003) as well as that of Opitom et al. (2019) is presented in Figure 3.

Fluxes are in ergs cm⁻² s⁻¹, and production rates are in molecules s⁻¹. Production rate ratios are rounded to the nearest tenth and are based on the 100 Å upper limit.

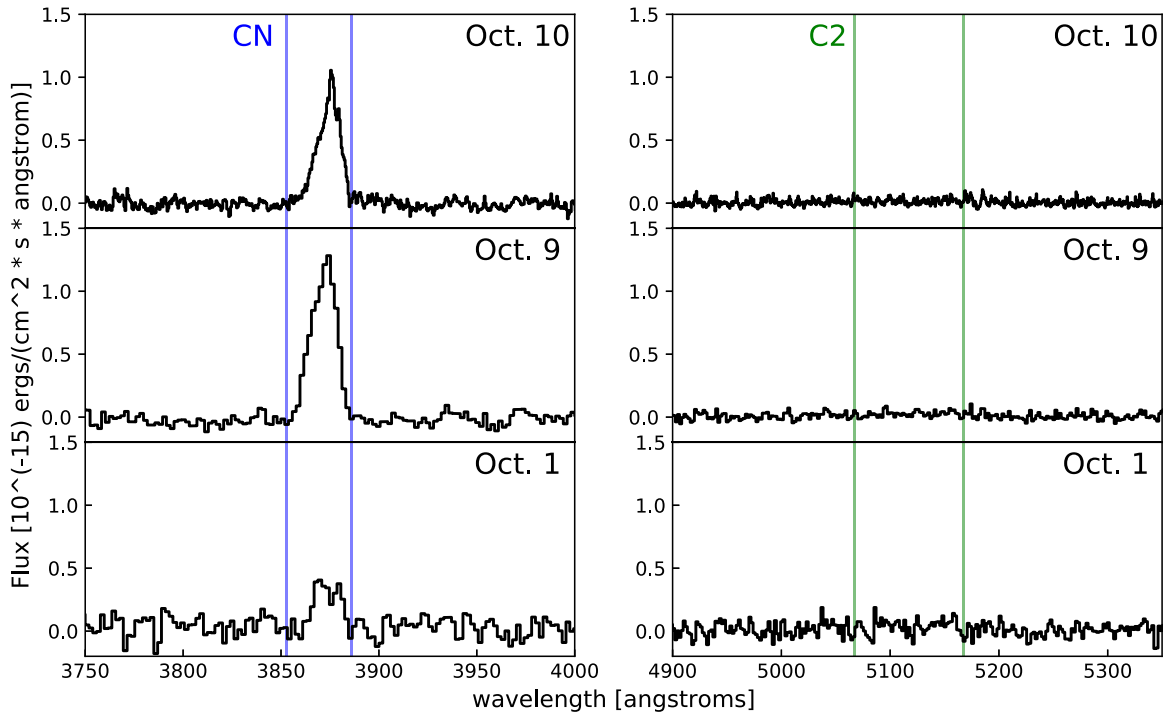


Figure 2. CN and C₂ spectral profiles at the MMT and LBT. The CN (left) and C₂ (right) spectral profiles from the spectra obtained between 2019 October 1 and October 10. Dotted horizontal lines are added to each plot to indicate the extraction spectral range, which we chose based on the extent of the line in the 2019 October 10 spectrum.

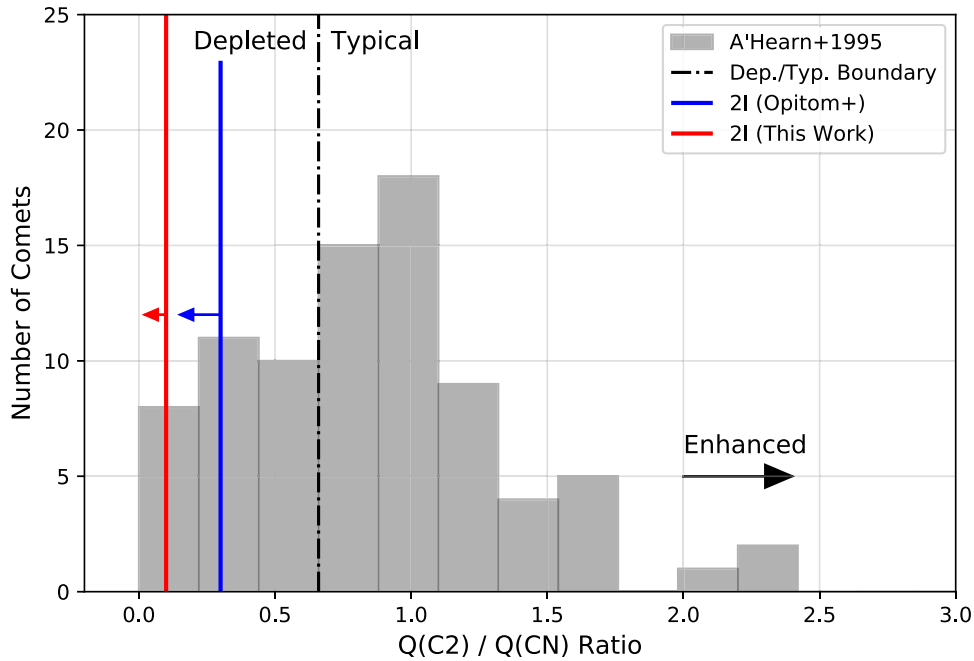


Figure 3. Taxonomical classification of 2I/Borisov. The ratio of production rates between C₂ and CN determined for 2I/Borisov (red line, red arrow) and the comets in the A’Hearn et al. (1995) survey that had their ratios determined (Osip et al. 2003). The upper limit from Opiotom et al. (2019) is presented similarly in blue. A black dashed–dotted line and text are present to differentiate between “Depleted” comets (ratio < 0.66) and “Typical” comets (ratio > 0.66) in the A’Hearn et al. (1995) taxonomy. “Enhanced” comets fall on the right and outside of the figure.

4. Discussion

4.1. 2I/Borisov as a Depleted Comet

Our further confirmation of CN emission, continuing nondetection of C₂ emission, and the lowest so far calculation of the $Q(C_2)/Q(CN)$ ratio provide a better framework than previously available to analyze 2I/Borisov in the context of

solar system comets. Our reported $Q(C_2)/Q(CN)$ upper limit (<0.1) is very low for solar system comets, with only three in the A’Hearn et al. (1995) sample being comparably depleted (43P/Wolf–Harrington: ~ 0.063 , 98P/Takamizawa: ~ 0.081 , and 87P/Bus: ~ 0.087). Only $\sim 34\%$ of the total comets with measured $Q(C_2)/Q(CN)$ ratios in that sample are depleted. We note that these detections are rather noisy and comparatively

old. $Q(C_2)/Q(CN)$ has also been observed to vary in 43P (Fink 2009) from very to mildly depleted. 19P/Borely also has a variable ratio (Fink 2009) that on one occasion was as low as ~ 0.06 . All of these lowest-ever detections are comparable to our upper limit. These ratios were all obtained at lower distances than the current measurements. The survey data sets also do not report every possible upper limit when a later detection could be reported, so the comparison is not without limitations. It is also unknown whether or not this ratio might change—it is possible that 2I/Borisov either has very little or no C_2 or that C_2 production might start at some later date.

In our solar system, Jupiter-family comets are the most likely to be depleted ($\sim 37\%$ versus $\sim 18\%$ for long-period comets, Cochran et al. 2012; $\sim 50\%$ versus $\sim 6\%$, A’Hearn et al. 1995) depending on the definition of depleted and the choice of dynamical classifications. Within this context, we might expect 2I/Borisov to have formed in a location more similar to many of the extremely depleted Jupiter-family comets, derived from the trans-Neptunian region, than the long-period comets, which likely formed near Uranus and Neptune. Inferences like this rest upon the assumption that the existing classification schemes are describing some underlying set of processes in the protosolar disk that created the modern properties and compositions of comets. More work is needed to understand if 2I/Borisov being carbon depleted has the same implications as it does in solar system comets. A reliable detection of the molecule C_2 in the spectrum of 2I/Borisov would help address this. C_2 and C_{33} are often but not always seen to be depleted, typical, or enriched in a similar manner (A’Hearn et al. 1995), suggesting strongly that their abundance is controlled by the same or similar processes. If C_3 is detected and is found to be correlated in production rate with C_2 , this would likely argue further that the taxonomies reflect some information about the chemical conditions in the disks where these objects formed. In other words, we would like the taxonomies based on solar system comets to be predictive for 2I/Borisov, instead of descriptive. Further spectroscopic monitoring of 2I/Borisov is needed for another reason; while production rate ratios (e.g., $Q(C_2)/Q(CN)$) are not observed to vary much with time or distance in solar system comets, we do not know if this is the case for 2I/Borisov as of yet. Again, it is worth emphasizing that C_2 production might truly be low or simply be low currently. While production rate ratios typically do not vary much in solar system comets, the surveys that found this were largely making observations when the comets in question were at lower heliocentric distance than those considered here. Continued monitoring will be critical to making the fullest comparison to solar system comets. If these diagnostic ratios are found to vary in 2I/Borisov, then our understanding of what our measurement of its strong depletion means would have to be revised greatly, if not thrown out altogether.

4.2. Comparison with Other Measurements

Our 2019 September 20 measurements took place approximately 7 hr after those of Fitzsimmons et al. (2019) and our $Q(CN)$ upper limit is slightly above their detection ($Q(CN) = (3.7 \pm 0.4) \times 10^{24}$, Fitzsimmons et al. 2019; $Q(CN) < 5.0 \times 10^{24}$, this work). Our later observations produce increasing CN production rates $((1.1\text{--}1.9) \times 10^{24}$ throughout 2019 October), which are wholly consistent with the results recently reported by Opitom et al. (2019). Considering the differences in instruments, reduction strategies, and modeling

approaches, we view this as good agreement with contemporary work that bolsters the validity of our approaches. Understanding how production rates vary with heliocentric distance is a critical goal for the upcoming observational campaign, as any deviations from normal cometary behavior might indicate some different mechanisms that regulate the release of gases from the interior of the object. While Opitom et al. (2019) argue based on their data that the trend in $Q(CN)$ is essentially flat, we again note that ours supports an increasing production rate over the same time period. We argue that the current data support the idea that 2I/Borisov is acting much like a normal solar system comet in this regard.

Both Fitzsimmons et al. (2019) and Opitom et al. (2019) placed upper limits on the $Q(C_2)/Q(CN)$ ratio (~ 1.0 and ~ 0.3 , respectively). Our upper limit is significantly below both, but our derived $Q(CN)$ production rates are statistically consistent. We view this as strong evidence that our derived upper limit is accurate.

Our dust reflectance slope measurements ($S' = 22\%/micron$ and $11\%/micron$ below and above the green continuum filter point at 5260 \AA from the Hale–Bopp filter set; Farnham et al. 2000) support the idea of Fitzsimmons et al. (2019) that the dust might be redder at shorter wavelengths. However, we note that small differences between measured reflectance slopes can be caused by a number of things, from different calibration methods to unknown instrumental artifacts, so more measurements are needed. A recent report (Yang et al. 2019, CBET 4672) has a somewhat shallower slope ($\sim 5\%$), for instance. This is a typical solar system value (see Guzik et al. 2019) and indicates dust with relatively similar reflective properties as that of solar system comets. The dust properties and general behavior of 2I/Borisov seem similar to many solar system comets, but its gas abundances might be very different.

5. Conclusions

We report on spectroscopic and imaging observations of 2I/Borisov between 2019 September 20 and 2019 October 26 using the Bok, MMT, and LBT telescopes to characterize and measure the gas production rates and dust reflectance properties to compare with solar system comets. We find the dust reflectance to be red ($S' = 22$ (11)/micron below (above) the Hale–Bopp green continuum filter) and likely shallower at larger wavelengths. We identify CN emission on all 2019 October dates and convert the integrated fluxes to production rates using a standard Haser model with a rectangular (for spectra) or circular (for imaging) aperture. From 2019 October 1 to 26, the production rate ranged from $Q(CN) = (1.1\text{--}1.9) \times 10^{24} \text{ mol s}^{-1}$ after our initial upper limit on 2019 September 20 ($Q(CN) < 5.0 \times 10^{24} \text{ mol s}^{-1}$). These values and dust reflectance properties are all consistent with contemporaneous observations by Fitzsimmons et al. (2019) and Opitom et al. (2019). We do not detect emission from C_2 on any date and set upper limits in the standard method of Cochran et al. (2012). For our most sensitive observations from the LBT on 2019 October 10, we find $Q(C_2) < 1.6 \times 10^{23}$ using a 100 \AA wide integration area. The ratio of C_2 to CN production rates was found on that date to be $Q(C_2)/Q(CN) < 0.1$, which is extremely depleted if any C_2 is even being produced at the current time. This ratio is used as a diagnostic measure of composition (e.g., “typical” or “depleted”; see A’Hearn et al. 1995; Fink 2009; Cochran et al. 2012), and only three solar system comets have been detected to be more

depleted than our upper limit. However, the comparability of our upper limit to detections in surveys with different goals is not ideal. It is unclear whether or not 2I/Borisov has little C₂, if any, or the C₂ it might have is simply not being released yet. More work is needed before we can truly apply a solar system classification onto 2I/Borisov and know that the statement has a physical meaning. More work is very much needed to further constrain this ratio and identify if 2I/Borisov has any long-chain hydrocarbons at all. The recent discovery of the interstellar comet 2I/Borisov presents an unparalleled opportunity to compare its composition to solar system comets and test the applicability of planetesimal formation models to other stellar systems.

We would like to congratulate Gennadiy Borisov on this great discovery and thank the IAU for letting the object retain his name as is typical for comets. We thank Kendall Sullivan among others for encouragement to pursue this project. We thank an anonymous reviewer for comments that greatly improved the Letter as well as Alan Fitzsimmons for very helpful correspondence on the topic. J.E.A. and N.S. receive support from NSF grant AST-1515559. K.V. acknowledges funding from NSF (grant AST-1824869). Some observations in this work were collected at Kitt Peak National Observatory; we are honored to be permitted to conduct astronomical research on Iolkam Du'ag (Kitt Peak), a mountain with particular significance to the Tohono O'odham Nation. Observations reported here were obtained at the MMT Observatory, a joint facility of the University of Arizona and the Smithsonian Institution. We appreciate the expertise of the Kitt Peak National Observatory, Steward Observatory, MMT Observatory, and LBT Observatory staff as well as Hannes Gröller who helped ensure the success of these observations.

This Letter made use of the modsIDL spectral data reduction pipeline developed in part with funds provided by NSF grant AST-1108693 and a generous gift from OSU Astronomy alumnus David G. Price through the Price Fellowship in Astronomical Instrumentation.

modsCCDRed was developed for the MODS1 and MODS2 instruments at the Large Binocular Telescope Observatory, which were built with major support provided by grants from the U.S. National Science Foundation's Division of Astronomical Sciences Advanced Technologies and Instrumentation (AST-9987045), the NSF/NOAO TSIP Program, and matching funds provided by the Ohio State University Office of Research and the Ohio Board of Regents. Additional support for modsCCDRed was provided by NSF grant AST-1108693.

Facilities: MMT(BCS), Bok (B&C, 90Prime), LBT (MODS).

ORCID iDs

Theodore Kareta  <https://orcid.org/0000-0003-1008-7499>
 Jennifer Andrews  <https://orcid.org/0000-0003-0123-0062>
 John W. Noonan  <https://orcid.org/0000-0003-2152-6987>
 Walter M. Harris  <https://orcid.org/0000-0002-8378-4503>
 Vishnu Reddy  <https://orcid.org/0000-0002-7743-3491>
 Kathryn Volk  <https://orcid.org/0000-0001-8736-236X>
 Albert Conrad  <https://orcid.org/0000-0003-2872-0061>

References

- A'Hearn, M. F., Feaga, L. M., Keller, H. U., et al. 2012, *ApJ*, **758**, 29
 A'Hearn, M. F., Millis, R. C., Schleicher, D. O., Osip, D. J., & Birch, P. V. 1995, *Icar*, **118**, 223
 Biver, N., & Bockelée-Morvan, D. 2016, in IAU Proc. 29A, Astronomy in Focus, ed. P. Benvenuti, 228
 Bar-Nun, A., & Kleinfeld, I. 1989, *Icar*, **80**, 243
 Belton, M. J. S., Hainaut, O. R., Meech, K. J., et al. 2018, *ApJL*, **856**, L21
 Bockelée-Morvan, D., & Biver, N. 2017, *RSPTA*, **375**, 20160252
 Chance, K., & Kurucz, R. L. 2010, *JQSRT*, **111**, 1289
 Cochran, A. L., & Schleicher, D. G. 1993, *Icar*, **105**, 235
 Cochran, A. L., Barker, E. S., & Gray, C. L. 2012, *Icar*, **218**, 144
 Dones, L., Brasser, R., Kaib, N., & Rickman, H. 2015, *SSRv*, **197**, 191
 Drahus, M., Guzik, P., Waniak, W., et al. 2018, *NatAs*, **2**, 407
 Duncan, M., Thomas, Q., & Scott, T. 1987, *AJ*, **94**, 1330
 Farnham, T. L., Schleicher, D. G., & A'Hearn, M. F. 2000, *Icar*, **147**, 180
 Fraser, W. C., Pravec, P., Fitzsimmons, A., et al. 2018, *NatAs*, **2**, 383
 Fink, U. 1992, *Sci*, **257**, 1926
 Fink, U. 2009, *Icar*, **201**, 311
 Fitzsimmons, A., Hainaut, O., Meech, K., et al. 2019, *ApJL*, **885**, L9
 Fitzsimmons, A., Snodgrass, C., Rozitis, B., et al. 2018, *NatAs*, **2**, 133
 Guzik, P., Drahus, M., Rusek, K., et al. 2019, arXiv:1909.05851
 Haser, L. 1957, *BSRSL*, **43**, 740
 Hastie, M., & Williams, G. G. 2010, *Proc. SPIE*, **7735**, 773507
 Hyland, M. G., Fitzsimmons, A., & Snodgrass, C. 2019, *MNRAS*, **484**, 1347
 Jewitt, D., & Luu, J. 2019, arXiv:1910.02547
 Knight, M. M., Protopapa, S., Kelley, M. S. P., et al. 2017, *ApJL*, **851**, L31
 León, J. D., Licandro, J., Serra-Ricart, M., et al. 2019, *RNAAS*, **3**, 131
 McKay, A. J., Cochran, A. L., Russo, N. D., & DiSanti, M. 2019, arXiv:191012785
 Meech, K. J., Weryk, R., Micheli, M., et al. 2017, *Natur*, **552**, 378
 Micheli, M., Farnocchia, D., Meech, K. J., et al. 2018, *Natur*, **559**, 223
 Mumma, M. J., Weissman, P. R., & Stern, S. A. 1993, in *Protostars and Planets III*, ed. E. H. Levy & J. I. Lunine (Tucson, AZ: Univ. Arizona Press), 1177
 Opitom, C., Fitzsimmons, A., Jehin, E., et al. 2019, *A&A*, **631**, L8
 Osip, D. J., A'Hearn, M., & Raugh, A. 2003, NASA Planetary Data System, EAR-C-PHOT-5-RDR-LOWELL-COMET-DB-PR-V1.0, NASA
 Pogge, R. W., Atwood, B., Belville, S. R., et al. 2006, *Proc. SPIE*, **6269**, 62690I
 Schleicher, D. G. 2010, *AJ*, **140**, 973
 Schleicher, D. G. 2008, *AJ*, **136**, 2204
 Trilling, D. E., Mommert, M., Hora, J. L., et al. 2018, *AJ*, **156**, 261
 Williams, G. G., Olszewski, E., Lesser, M. P., & Burge, J. H. 2004, *Proc. SPIE*, **5492**, 787
 Yang, B., Kelley, M. S. P., Meech, K. J., et al. 2019, arXiv:1912.05318